Aalborg Universitet

AALBORG UNIVERSITY

Effect of thermal loading definitions on the mission profile-based reliability evaluation of power devices in PV inverters

Ryu, Taerim; Choi, Ui-Min; Vernica, Ionut; Blaabjerg, Frede

Published in:
Microelectronics Reliability

DOI (link to publication from Publisher):
10.1016/j.microrel.2022.114650

Creative Commons License
CC BY-NC-ND 4.0

Publication date:
2022

Document Version
Accepted author manuscript, peer reviewed version

Link to publication from Aalborg University

Citation for published version (APA):
Ryu, T., Choi, U.-M., Vernica, I., & Blaabjerg, F. (2022). Effect of thermal loading definitions on the mission profile-based reliability evaluation of power devices in PV inverters. *Microelectronics Reliability*, *138*, 1-5. Article 114650. https://doi.org/10.1016/j.microrel.2022.114650

General rights
Copyright and moral rights for the publications made accessible in the public portal are retained by the authors and/or other copyright owners and it is a condition of accessing publications that users recognise and abide by the legal requirements associated with these rights.

- Users may download and print one copy of any publication from the public portal for the purpose of private study or research.
- You may not further distribute the material or use it for any profit-making activity or commercial gain
- You may freely distribute the URL identifying the publication in the public portal -

Take down policy
If you believe that this document breaches copyright please contact us at vbn@aub.aau.dk providing details, and we will remove access to the work immediately and investigate your claim.

Effect of thermal loading definitions on the mission profile-based reliability evaluation of power devices in PV inverters

Taerim Ryu [a], Ui-Min Choi [a,*], Ionut Vernica [b] and Frede Blaabjerg [b]

[a] *Department of Electronic and IT Media Engineering, SeoulTech, Seoul, South Korea*
[b] *AAU Energy, Aalborg University, Aalborg, Denmark*

Abstract

The long-term mission profile-based lifetime evaluation of a PV inverter plays an important role in the Design for Reliability approach to ensure the required reliability performance. In previous studies, different thermal loading definitions have been considered for the mission profile-based lifetime estimation of power devices. It may affect the reliability prediction result considerably but its impact has not yet been studied. In this paper, the effect of thermal loading definitions on the predicted reliability of power devices in a PV inverter is investigated. The thermal loadings and reliability of power devices of a single-phase five-level T-type inverter by considering four different thermal loading definitions are comparatively analyzed and further discussed. Finally, some guidelines for selecting the thermal loading definition are suggested.

1. Introduction

The mission profile-based lifetime evaluation of a PV inverter plays an important role in the Design for Reliability approach (DfR) to ensure the required reliability performance [1]. Therefore, much research has been performed about it with a focus on reliability-critical components such as power devices and capacitors.

The thermal loading of power devices is one of the main causes of wear-out failure and it is strongly dependent on the PV power generation determined by mission profiles at installation sites [2,3]. Therefore, for the lifetime evaluation, typically long-term mission profiles of PV systems with various time resolutions ranging from a few minutes to several tens of minutes are considered with lifetime models with respect to temperature stress [3-8].

In the previous studies, different thermal loading definitions have been applied to obtain the required stress factors of lifetime models for the lifetime estimation such as junction temperature swing (ΔT_j), mean junction temperature (T_{jm}), and heating time (t_{on}). In [3,4], the change of mean junction temperature (T_{jmean}) due to the change in operating conditions under the mission profile is considered as the thermal loading, where the junction temperature variation ($\Delta T_{j(60Hz)}$) because of the line frequency power cycling is neglected. In [5,6], the impact of junction temperature variation caused by the line frequency power cycling is also considered as thermal loading, and therefore, the damages due to them are accumulated additionally. In [7,8], the change of maximum junction temperature (T_{jmax}) is taken into account instead of T_{jmean} without consideration of $\Delta T_{j(60Hz)}$. The literature that considers both the change of T_{jmax} and variation of T_j caused by the line frequency power cycling has not been found. The thermal loading definitions may affect the mission profile-based reliability prediction result considerably, but its impact has not yet been studied.

In this paper, to address this issue, the effect of thermal loading definitions on the reliability prediction of a PV inverter is investigated. The thermal loadings and reliability of power devices of a single-phase five-level T-type inverter based on the annual mission profile by considering four different thermal loading definitions are comparatively analyzed and further discussed. Finally, some guidelines for selecting the thermal loading definition are suggested.

2. Photovoltaic System

2.1. Configuration of PV system

In this study, as shown in Fig. 1, the reliability of the power devices of the PV inverter of a single-

* Corresponding author. uch@seoultech.ac.kr
Tel: +82 (10) 4156 4994

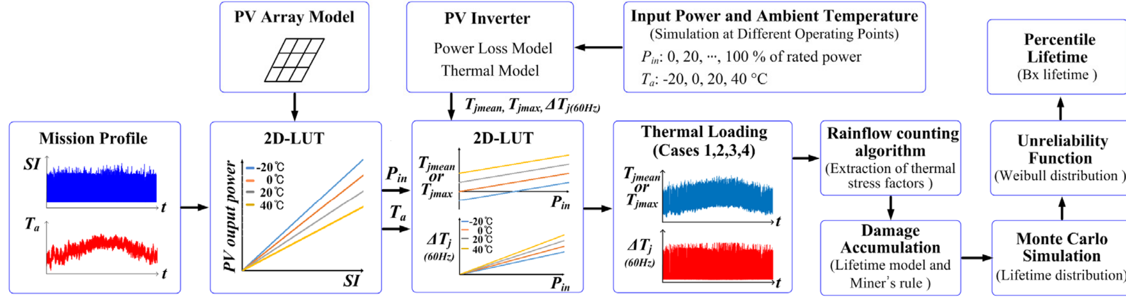

Fig. 3. Mission profile based lifetime evaluation procedure of the power devices of PV inverter: P_{in} – input power, T_a – ambient temperature, SI – solar irradiance, LUT – lookup table, T_{jmean} – mean junction temperature, T_{jmax} –maximum junction temperature, $\Delta_{Tj(60Hz)}$ – junction temperature swing due to line-frequency power cycling.

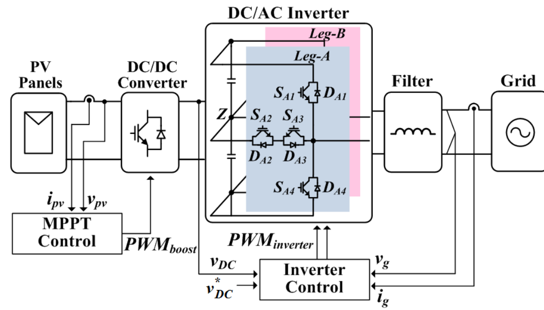

Fig. 1. Configuration of a single-phase PV System.

Table 1
Parameters of the PV system

Parameter	Value
Rated Power (P_{out})	7 kW
DC-link voltage (V_{DC})	400 V
Switching frequency (f_{sw})	20 kHz
Grid phase voltage (v_g)	220 V_{rms}
Grid frequency (f_g)	60 Hz
Capacitance (C)	2200 μF
Filter Inductor (L)	2 mH
IGBT module	10-12NMA040SH-M267F

phase PV system is the main focus, where the bond-wire failure of the IGBTs used in a single-phase five-level T-type NPC topology is considered. It is also assumed that the Unipolar Pulse Width Modulation is applied. Its related parameters are listed in Table 1. The cooling system is typically designed so that the T_{jmax} at the rated power is about 70-80 % of the rated junction temperature. To satisfy this condition, the thermal resistance between heat-sink and ambient ($R_{th(h-a)}$) is set to 0.18 K/W in this case study.

2.2. Mission profiles of PV system

Solar irradiation and ambient temperature (T_a) are typically considered as mission profiles of PV systems because the PV power generation is mainly dependent on them.

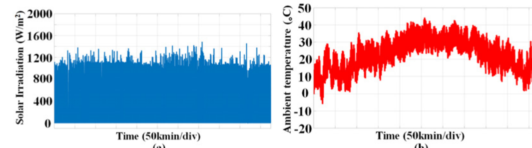

Fig. 2. Mission profiles of PV system recorded in Arizona in USA for one year.

In the previous studies [3-8], the long-term mission profiles such as one year having a range of time resolutions of a few minutes (e.g. 1-10 min) have been commonly applied for the reliability analysis of PV inverters. In this study, an annual mission profile recorded in Arizona (USA) with a sampling rate of 1 minute/sample, as shown in Fig. 2 is considered.

3. Lifetime evaluation based on mission profile

The procedure to estimate the lifetime of the power devices based on mission profile is shown in Fig. 3 and explained as follows.

3.1. Translation of mission profile into thermal loading

The input power and voltage of the PV inverter are determined by applying the mission profile to the PV module model. After that, the power loss of the power device is calculated and applied to the thermal model of the power device to estimate the junction temperature (T_j) at a certain operating condition. More detailed information to obtain the power loss and junction temperature can be found in [6,7].

The power loss distribution and corresponding junction temperatures at the rated power of 7 kW with 40 °C of T_a are shown in Fig. 4 and Fig. 5, respectively. It is seen that the power losses of S_{x1} and S_{x4} are dominant and therefore, they have the highest junction temperature of 104 °C.

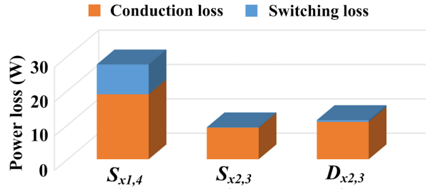

Fig. 4. Power loss distributions of the T-type NPC inverter at the rated power of 7 kW.

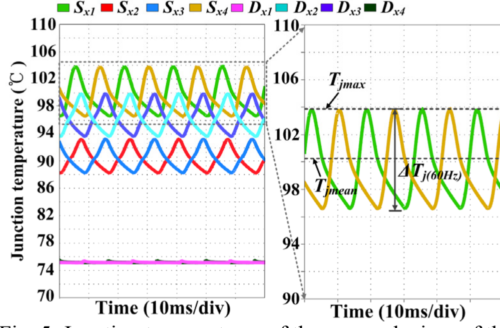

Fig. 5. Junction temperatures of the power devices of the T-type NPC inverter at 7 kW.

Based on the simulation results at the different operating points, a look-up table in connection with input power and ambient temperature is made with regard to T_{jmean} or T_{jmax}. The other one is also built with respect to $\Delta T_{j(60Hz)}$. Then, the thermal loadings of power devices during the given mission profile are acquired through the look-up tables when the determined input power and T_a are given, which is helpful to handle long-term mission profile-based simulations. The definitions of T_{jmean}, T_{jmax}, and $\Delta T_{j(60Hz)}$ can be found in Fig. 5.

Based on the above two lookup tables, four different cases of thermal loadings are defined and taken into account in this study as

1) Case 1: Change of T_{jmean} due to the change in operating conditions under the mission profile [3,4].

2) Case 2: Change of T_{jmax} due to the change in operating conditions under the mission profile [7,8].

3) Case 3: Change of T_{jmean} + variation of T_j due to line frequency power cycling [5,6].

4) Case 4: Change of T_{jmax} + variation of T_j due to line frequency power cycling.

The way to define the stress factors from the different thermal loadings and the thermal loadings of S_{A1} based on four thermal loading definitions are shown in Figs. 6 and 7, respectively.

3.2. Accumulated damage under different thermal loading definitions

There are representatively two kinds of thermal loadings due to variation in T_{jmean} or T_{jmax} called low-

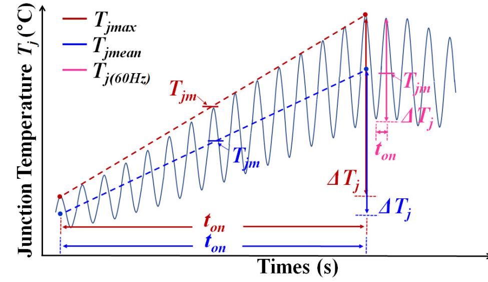

Fig. 6. Thermal stress factors of lifetime model for lifetime estimation under different thermal loading definitions.

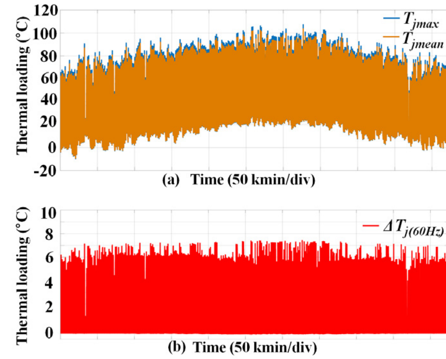

Fig. 7. Thermal loadings of S_{A1} depending on the thermal loading definitions (a) variation in T_{jmean} and T_{jmax} (b) line frequency power cycling.

frequency power cycling and due to variation in T_j caused by the line frequency power cycling. Since the low-frequency power cycling is irregular during the mission profile, a Rainflow counting algorithm is used to extract the thermal stress factors of junction temperature swing (ΔT_j), minimum (T_{jmin}) or mean junction temperature (T_{jm}), and heating time (t_{on}) from the thermal loadings. The number of cycles to failure (N_f) at the given combination of thermal stress factors is calculated by putting them into a lifetime model. In this study, the lifetime model presented in [9] is used for the case study as

$$N_f = A \cdot \left(\Delta T_j\right)^{-\beta_1} \cdot \exp\left(\frac{\beta_2}{T_{jmin}+273}\right) \cdot \left(t_{on}\right)^{\beta_3} \cdot I^{\beta_4} \cdot V^{\beta_5} \cdot D^{\beta_6} \quad (1)$$

The parameters values for the lifetime model can be obtained from [9].

The accumulated damage (AD) of power devices is calculated based on the Miner's rule as

$$AD = \sum_{i=1}^{k} \frac{n_i}{(N_f)_i} \quad (2)$$

where n_i is the number of cycles accumulated at a certain thermal stress (S_i) which is the combination of thermal stress factors of ΔT_j, T_{jmin}, and t_{on} and $(N_f)_i$ is the number of cycles to failure at S_i determined from the lifetime model. If the damage is accumulated such that AD = 1, it is considered that the power device is reached its end-of-life.

It is worthwhile mentioning that the t_{on} is limited to 60 s in this under the assumption that the viscoplastic deformation is saturated for a t_{on} > 60 s [10, 11]. Therefore, if the t_{on} is more than 60 s, the value of the t_{on} in the lifetime model is fixed to 60 s. However, if a lifetime model which is validated for more than a t_{on} of 60 s is available, the longer t_{on} can be applied.

Another type of damage is from the T_j variation due to the line frequency power cycling between sampling intervals of the mission profile. The AD per every minute is expressed as

$$AD = \sum_{i=1}^{k} \frac{n_{i,60}}{(N_f)_i} = \sum_{i=1}^{k} \frac{60 \times 60}{(N_f)_i} \tag{3}$$

where $n_{i,60}$ denotes the number of 60 Hz power cycling in one minute. The t_{on} of the thermal loading due to line frequency power cycling is 1/120 s since the line frequency is 60 Hz. However, it is far below the range of t_{on} of the considered lifetime model. Therefore, in order to further extend the validity of the range of t_{on}, a derating factor has been considered in previous research [5, 6] given as below

$$\frac{N_f(t_{on})}{N_f(1.5\text{s})} = \left(\frac{t_{on}}{1.5\text{s}} \right)^{-0.3} \tag{4}$$

where $N_f(t_{on})$ is the number of cycles to failure under the obtained heating time t_{on} and N_f(1.5 s) is the N_f when the t_{on} is 1.5s.

The accumulated damages of the power devices of single-phase T-type NPC inverter during the mission profile under the four cases of thermal loading definitions are summarized in Table 2. It can be seen that the S_{x1} and S_{x4} are the most reliability-critical components since they have the highest AD and thus play a key role in the reliability of the T-type NPC inverter. Furthermore, there are significant increases in AD when the thermal loadings due to line frequency power cycling are taken into account. In the case of S_{x1} and S_{x4}, AD increases about 111 % and 92 % from Case 1 to Case 3 and from Case 2 to Case 4, respectively. Therefore, it can be expected that the lifetime might be significantly different.

Table 2
Accumulated damage of power devices (See Fig.1)

Power device	Accumulated Damage (×10^{-3})			
	Case 1	*Case 2*	*Case 3*	*Case 4*
$S_{x(x=A,B)1,4}$	5.79	7.25	12.25	13.90
$S_{x2,3}$	3.15	3.78	4.40	5.05
$D_{x2,3}$	4.99	6.15	9.86	11.16

3.3. System-level reliability evaluation

The Monte Carlo simulation is performed to have the lifetime distributions of the power devices for the reliability functions. It is implemented with a population of 10,000 samples, where a 5 % variation in the lifetime model parameters and equivalent thermal stresses are considered according to previous research. A more detailed explanation of the Monte Carlo simulation can be found in [3-8].

The lifetime distribution of each power device from the Monte Carlo simulation is fitted with the Weibull distribution. Then, the cumulative density function called unreliability function is obtained which is expressed as

$$F(t) = \int_0^t f(x)\,dx, \text{and } f(t) = \frac{\beta}{\eta}\left(\frac{t}{\eta}\right)^{\beta-1} e^{-\left(\frac{t}{\eta}\right)^{\beta}} \tag{5}$$

where $F(t)$ and $f(x)$ are the cumulative density function and probability density function of the Weibull distribution, respectively. t, β and η are the operating time, shape parameter and scale parameter, respectively.

Since the individual power device failure cause the overall inverter failure, based on the reliability block diagram approach, the unreliability function of the entire inverter system $F_{inv}(t)$ is represented as

$$F_{inv}(t) = 1 - \prod_{k=1}^{n} \left(1 - F_k(t)\right) \tag{6}$$

where $F_k(t)$ is the unreliability of the k_{th} power device in the T-type NPC inverter.

From the unreliability function, the percentile lifetime (B_X lifetime) that indicates the lifetime of a population of items is obtained. For example, B_1 lifetime is the time by which failure in 1 % of items occurs. Namely, the reliability is 0.99.

The unreliability functions of the T-type NPC inverter considering all power devices and the corresponding B_1 lifetimes under four cases of thermal loading definitions are shown in Fig. 6.

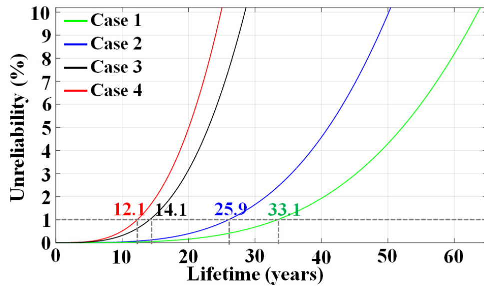

Fig. 6. System-level unreliability functions and the corresponding B_1 lifetimes.

When the changes of T_{jmean} and T_{jmax} are considered as the thermal loadings, which are Case 1 and Case 2, the B_1 lifetimes are 33.1 and 25.9 years, respectively. The B_1 lifetime is decreased by more than a half when the T_j variation due to line frequency power cycling is considered as thermal loadings additionally, which are Case 3 and Case 4 and B_1 lifetimes are 14.1 and 12.1, respectively.

As it is seen from the results, the lifetime estimation result is considerably affected by the thermal loading definitions, and thus care must be taken during the reliability assessment based on the long-term mission profile.

4. Discussion and Conclusion

In thermal loading-based lifetime estimation of power devices, it assumes that temperature variation leads to the expansion and contraction of materials and thus applies the mechanical forces at the point of contact of different materials in the modules. If the applied stress is below the yield strength of the material, elastic deformation occurs that may not result in permanent damage. However, plastic deformation occurs if it is above the yield strength, which causes permanent damage. In [12], a threshold of the ΔT_j between elastic and plastic regions is investigated. As the T_{jmean} increases, the magnitude of ΔT_j for plastic deformation decreases, but it is more than 20 °C of ΔT_j within a normal operating range. Therefore, it can be expected that the small temperature variations may lead to elastic deformation and, therefore, their impacts on the wear-out failure are insignificant. It should be noted that the threshold of the ΔT_j will be different for other kinds of power modules. However, in much previous research, the effect of small junction temperature variation is included unrestrictedly. It may lead to an overestimation of the accumulated damage and thus shorter estimated lifetime. In this study, the T_j variations due to line frequency power cycling are less than 8 °C. When they are included as thermal loadings, which are Cases 3 and 4, the lifetime is shortened by more than a half compared to the results excluding it. Furthermore, according to [7], too short t_{on}, which means very fast transient, the temperature does not propagate through different materials layers. Therefore, it does not have an impact on device damage.

Consequently, based on the above discussion and lifetime analysis results, the followings are recommended:

1) The thermal loadings caused by the T_j variation due to line frequency power cycling should be excluded for the lifetime estimation since it is typically below 10 °C, which means that it would be in the elastic stress range.
2) If ΔT_j value due to line frequency power cycling is in the plastic stress range, for example, above 20 °C, it should be included for the lifetime estimation regarding bond-wire failure but should be excluded for regarding baseplate solder-joint failure since the temperature cannot propagate to it sufficiently with short transient time.
3) For the thermal loading definition, the change of T_{jmax} (i.e. Case 2) is more recommended than the change of T_{jmean} (i.e. Case 1) since it is the actual maximum temperature that the junction is reached.

However, it is difficult to set a precise threshold of ΔT_j for plastic deformation and also a limit of t_{on} for each module experimentally since the power cycling test needs to be performed for a long time with low-temperature variation ranges. Therefore, further investigation based on physics-of-failure is still required. Nevertheless, the proper limit of the ΔT_j must be considered when the mission profile-based lifetime estimation is performed to prevent the excessive underestimation of the reliability of power devices in inverter systems.

Acknowledgements

This study was supported by the Research Program funded by the Seoul National University of Science and Technology.

References

[1] J.M. Lenz, et al., Mission profile characterization of PV systems for the specification of power converter design requirements, *Sol. Energy*, vol. 157, pp. 263–276, 2017.

[2] M. Andresen, et al., Thermal stress analysis and MPPT optimization of photovoltaic systems, *IEEE Trans. Ind. Electron*., vol. 63, no.8, pp.4889–4898, Aug. 2016.

[3] A. Sangwongwanich, et al., “Lifetime Evaluation of Grid-Connected PV Inverters Considering Panel Degradation Rates and Installation Sites,” *IEEE Trans. on Power Electron.*, vol. 33, no. 2, pp. 1225-1236, Feb. 2018.

[4] A. Anurag, et al., “Thermal Performance and Reliability Analysis of Single-Phase PV Inverters With Reactive Power Injection Outside Feed-In Operating Hours,” *IEEE J. Emerg. Sel. Topics Power Electron.*, vol. 3, no. 4, pp. 870-880, Dec. 2015.

[5] P. D. Reigosa, et al., “Prediction of Bond Wire Fatigue of IGBTs in a PV Inverter Under a Long-Term Operation,” *IEEE Trans. on Power Electron.*, vol. 31, no. 10, pp. 7171-7182, Oct. 2016.

[6] J. He, et al., “Lifetime Evaluation of Three-Level Inverters for 1500-V Photovoltaic Systems,” *IEEE J. Emerg. Sel. Topics Power Electron.*, vol. 9, no. 4, pp. 4285-4298, Aug. 2021.

[7] U. M. Choi and T. Ryu, “Comparative Evaluation of Efficiency and Reliability of Single-Phase Five-Level NPC Inverters for Photovoltaic Systems,” *IEEE Access*, vol. 9, pp. 120638-120651, 2021.

[8] U. M. Choi and J. S. Lee, “Single-Phase Five-Level IT-Type NPC Inverter with Improved Efficiency and Reliability in Photovoltaic Systems,” *IEEE J. Emerg. Sel. Topics Power Electron.*, doi: 10.1109/JESTPE.2021.3103252.

[9] R. Bayerer, et al., “Model for Power Cycling lifetime of IGBT Modules – various factors influencing lifetime,” *in Proc. of CIPS 08*, pp. 1-6, Mar. 2008.

[10] Infineon. 2019. PC and TC Diagrams. [Online]. Available: https://www.infineon.com

[11] I. Paul, et al., “Application based modified reliability tests and their physical correlation with lifetime assessment models,” *in Proc. Int. Conf. Power Electron., Intell. Motion, Power Qual. Energy Manage. (PCIM Eur.)*, May 2013, pp. 557–563.

[12] S. Hartmann et al., “Bond wire life time model based on temperature dependent yield strength,” *in Proc. Int. Conf. Power Electron., Intell. Motion, Power Qual. Energy Manage. (PCIM Eur.)*, May 2012, pp. 494–501.